Sensors and Actuators B 177 (2013) 818–825

Contents lists available at SciVerse ScienceDirect

Sensors and Actuators B: Chemical

journal homepage: www.elsevier.com/locate/snb

Aptamer-gold nanoparticle-based colorimetric assay for the sensitive detection of thrombin

Yi Peng, Lidong Li*, Xiaojiao Mu, Lin Guo*

Key Laboratory of Bio-Inspired Smart Interfacial Science and Technology of Ministry of Education, School of Chemistry & Environment, Beijing University of Aeronautics & Astronautics, Beijing 100191, PR China

ARTICLE INFO

Article history:
Received 5 October 2012
Received in revised form
29 November 2012
Accepted 1 December 2012
Available online 10 December 2012

Keywords:
Thrombin
Nanoparticles
Aptamer
Biosensor
UV–vis

ABSTRACT

Herein, we report a sensitive and selective detection method for thrombin based upon oligonucleotide-functionalized gold nanoparticle probes that can combine with the thrombins by van der Waals force, where the thrombin molecule acts as a bridge to link the monodispersed aptamer-modified gold nanoparticles together, since thrombin includes two binding sites for the aptamer. This leads to the visible color changes from wine-red to blue-purple, which relies upon the distance-dependent optical properties of gold nanoparticles. The concentration can be determined by monitoring with naked eye or a UV–vis spectrometer. In addition, this assay does not utilize any organic cosolvents, heavy metal ion, enzymatic reactions, light-sensitive dye molecules, lengthy protocols, or sophisticated instrumentation, thereby overcoming some limitations of more conventional methods. Moreover, thrombin at concentrations as low as 5 pM (1.679 ng/mL) can be detected in this assay with a colorimetric format.

1. Introduction

To date, nanomaterials have been widely used in medical science, pharmacology, chemistry, bioassay, manufacture, photology, energy of source, national defense and etc. Among all the nanometer materials, gold nanoparticles (AuNPs) have attracted tremendous attention due to their unique optical properties, robust nature, stability, and their large surface areas. Benefiting from these advantages, AuNPs can consequently be applied to biosensors in molecular recognition, disease detection, and clinical therapy. These excellent features provide AuNPs-based assay clear superiorities over other methods for nucleic acid and protein detection, as shown in certain pioneer studies [1].

As a new class of single-stranded DNA/RNA molecules, aptamers are short nucleic acid ligands artificially selected for their high specificity and affinity for a wide range of target molecules including proteins, drugs, small molecules, inorganic ions and even cells [2]. They are excellent recognition molecules for numerous reasons, for example, the ease of aptamer production, storage, and modification; their small size and chemical simplicity; their target versatility; and their relative resistance to denaturation and degradation [3–5]. Thus, they have wide applications in medical diagnosis [6], environmental monitoring [7], and biological analysis [8,9].

Thrombin is one of the ubiquitous proteins in mammals which is an endoprotease that naturally functions as a blood clotting factor to convert fibrinogen to fibrin both under physiological conditions and in a pathological thrombus [10]. Also, thrombin has some properties similar to hormone, and is relevant to thrombosis and platelet activation. Therefore, thrombin plays an important role in lists of cardiovascular diseases [11], and it is reported to regulate many processes in inflammation and tissue repair at the blood vessel wall. As the higher concentration of thrombin in blood is known to be relevant with some diseases, cancer [6], for example, it is significant to be able to detect this enzyme accurately at trace levels with high sensitivity. So far, numerous approaches to detect thrombin have been developed, for instance, fluorescence [12,13], surface enhanced Raman spectroscopy (SERS) [14,15], and electrochemistry [16–18]. Most of them, however, require complicated instrumentation; involve cumbersome laboratory procedures, which limits the scope of their practical applications. Some of them also suffer by the disadvantages, such as relatively high detection limits, narrow detection range, and expensive labeling substances.

Recently, significant advances have been made in the development of chromophoric colorimetric sensors for detecting proteins, oligonucleotides and small inorganic molecules [1,19–32]. They have attracted tremendous attention due to their easy readout (often with the naked eye) and potential for high throughput formats. To date, biomaterial-metallic nanoparticle hybrid systems

* Corresponding authors. Tel.: +86 010 82338162; fax: +86 010 82338162.
E-mail addresses: lilidong@buaa.edu.cn, xhlili@163.com (L. Li), guolin@buaa.edu.cn (L. Guo).

0925-4005/$ – see front matter © 2012 Elsevier B.V. All rights reserved.
http://dx.doi.org/10.1016/j.snb.2012.12.004

Table 1
Summary of aptamer-based thrombin sensors.

Sensor conjunction	Method	LOD[a]	Linear range	Reference
Au/SH-TBA/TB/TBA/AuNP/Raman Probe/AgNP	SERS	0.5 nM	Not given	Shuman and Majerus [33]
Si substrase/AuNPs/SH-TBA(-FITC)/TB	SERS	20 pM	0.1–10 pM	Hu et al. [14]
TBA/TA + TASPI	Fluorescence	50 nM	0.05–2.5 μM	Wang et al. [34]
QD/NH-TBA/TB + BOBO-3	Fluorescence	1 nM	1–500 nM	Yan et al. [35]
Magnetic bat/eletrode/AuMNP/SH-Apt1/TB/SH-Apt2-CS-AuNPs-HRP	Electrochemical	5.5 fM	0.01–10 pM	Chi et al. [36]
Electrode/nafion@graphene/MB/AuNPs/SH-TBA(BSA)/TB	Electrochemical	6 pM	0.01–50 nM	Zhao et al. [37]
TB/TBA/hemin complex(ABTS-H_2O_2)	Colorimetric/absorbance	20 nM	0.02–2 μM	Sun et al. [38]
Nanorose/SH-Apt15/TB/SH-Apt29/nanorose	Colorimetric/absorbance	1 nM	1.6–30.4 nM	Liang et al. [39]
AuNP/SH-TBA/TB/SH-TBA/AuNP	Colorimetric/absorbance	5 pM	0.005–100 nM	This work

[a] LOD: limit of detection.

are extensively used in different bioanalytical applications. AuNPs, coupled to aptamers were employed as active units in different biosensing systems. The specific aptamer–protein interactions were employed to develop label-free biosensors. Herein, we report a new approach of colorimetric determination of thrombin based upon aptamer-functionalized AuNPs aggregates. Since thrombin includes two binding sites for the aptamer, the thrombin-induced aggregation of the AuNPs is anticipated, which results in the colormetric change directly observed from the naked eyes. These target-induced DNA-linked AuNPs network structures have shown great promise for detecting other molecules, which have two binding sites with their aptamers. As compared to the performance of several prevalent aptamer-based thrombin sensors (as shown in Table 1), the proposed method has some obvious advantages. First of all, our method has relatively wider linear range and a lower detection limit. Second, our method is one of the few that protein can be detected by the simple "mix and detect" fashion, which greatly decreases the operating difficulty, but most of the previous methods have relative complicated steps. In addition, the instrumentation required for this method is inexpensive and simple, while the SERS or fluorescence methods need expensive and complex facilities. Taken all together, our method presented here is highly desirable, because it is not only fast, sensitive and reliable but also simple, practical, and economical in its operation. Therefore, it has great potential in the application of other protein detections, which have two or more binding sites with their aptamers.

2. Experimental

2.1. Chemicals and materials

The synthetic anti-thrombin oligonucleotides, single stranded DNA (ssDNA) (5′-(SH)-$(CH_2)_6$-CCA TCT CCA CTT GGT TGG TGT GGT TGG-3′) were obtained from TaKaRa Biotechnology (Dalian, China) Co., Ltd. α-Thrombin form lyophilized erythrocytes were purchased from Sigma–Aldrich (USA), and lysozyme(Ly), bovine serum albumin(BSA), bovine hemoglobin(BHb) form lyophilized erythrocytes were purchased from CNS Bioservices (Beijing, China) Co., Ltd. Tris-(2-carboxy-ethyl) phosphine hydrochloride (TCEP) was obtained from Alfa-Aesar (Tianjing, China). Sodium tetrachloroaurate (III) ($HAuCl_4$), sodium citrate, were purchased from Sigma–Aldrich (USA). All other reagents were of analytical reagent grade. All solutions were prepared with doubly distilled water (pH = 7.0).

2.2. Instrumentation

UV–vis spectrophotometer was provided by Shanghai Lap-Spectrum Instruments (Shanghai, China) Co., Ltd.

2.3. Synthesis of AuNPs

Gold nanoparticles (AuNPs) were prepared by citrate reduction of $HAuCl_4$ in aqueous solution according to the literature [4,40]. The size of nanoparticles was characterized by Transmission Electron Microscopy (TEM) photographs, X-ray Diffraction (XRD), and UV–Vis spectrophotometry. Average particle diameters were consistently in the range of 13.3 nm with standard deviations of 1.2 nm [41,42]. The concentration of the AuNPs was estimated to be 15 nM, which was determined according to the Beer's law by using the extinction coefficient of 10^8 M^{-1} cm^{-1} for 13.3 nm AuNPs in diameter at 520 nm [4,26]. XRD experiments were also carried out to investigate the purity and size distribution of the sample (data not shown). By the Debye–Scherrer equation, the calculated diameter of AuNPs is in good agreement with the result from the TEM.

2.4. Preparation of aptamer-modified AuNPs

The thiol-modified 27-mer DNA oligonucleotides (anti-thrombin aptamer) were attached to the AuNPs as follows: 100 μM aptamers heated to 90 °C and gradually cool to room temperature. This heating and cooling step helps to maintain the structural flexibility of the aptamers (for binding thrombin). 1 μL TCEP solution (1 mM) and 99 μL anti-thrombin aptamer with different concentrations (50 nM and 500 nM were used in this article) were mixed together and kept at room temperature for half an hour to ensure the disulfide cleavage finished completely. Herein, TCEP is a reducing agent, which is intended to disrupt any disulfide bonds (—S—S—) and ensures that the free —SH groups are ready to react with the gold surface [43,44]. Afterwards, 60 μL AuNPs and 10 μL aptamer (thiol modified DNA) with different concentrations were mixed together and kept at room temperature for 16 h. During this time, the aptamers were wrapped in AuNPs (Scheme 1b) by strong covalent bond between —SH and gold.

2.5. Aggregation assays

2 μL thrombins were accumulatively added to the aptamer-modified AuNPs solution (70 μL) to make the final concentration of thrombin ranging from 5 pM–500 nM. After mixing in the sonicator for a few seconds carefully, the mixture was maintained at 37 °C in the incubator for half an hour. During this time, thrombin and the Apt-AuNPs were combined together by the van der Waals forces. Since thrombin includes two binding sites for the aptamer, thrombin molecule acts as a bridge (supporting information gives a detailed discussion) to link the monodispersed aptamer-modified gold nanoparticles together to make the aggregation (Scheme 1c). During the interaction, the aptamer formed a G4 structure (as shown in Scheme 2). All solutions were placed into 100 μL quartz cuvette, and their absorbance was measured using a UV–vis spectrophotometer.

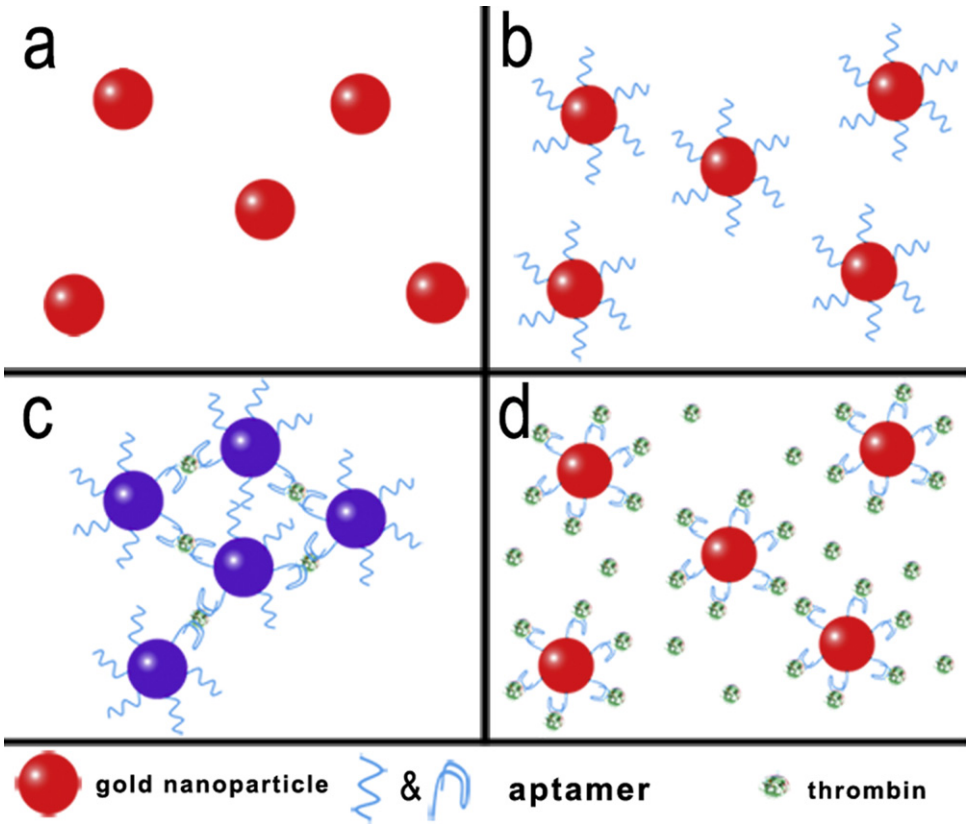

Scheme 1. Schematic representation of the detection mechanism: (a) monodispersed gold nanoparticles and (b) gold nanoparticles modified with aptamers. The aggregation of aptamer-AuNPs in the presence of thrombins at: (c) lower concentration and (d) higher concentration. Aggregation of the Apt-AuNPs occurred at lower concentration of thrombin, but the AuNPs aggregates dispersed at higher concentration.

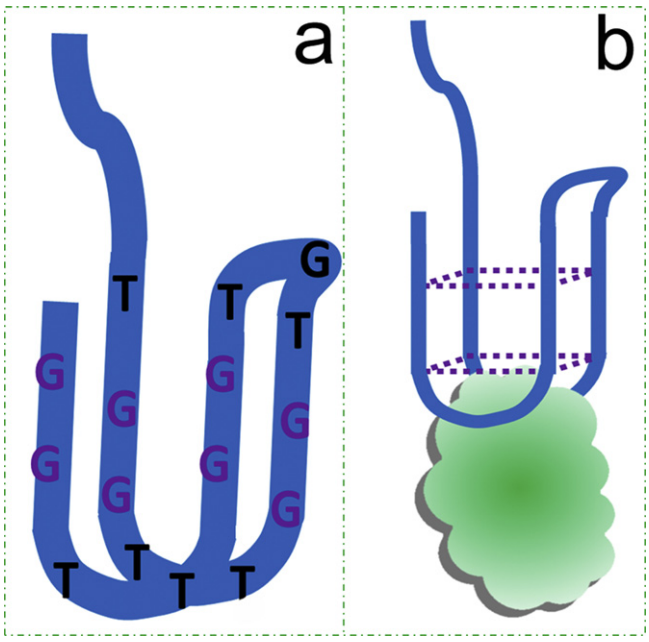

Scheme 2. Schematic representations of (a) the secondary structure of DNA when binding with thrombin (9 Gs and 6 Ts are marked in purple and black respectively). (b) The binding structure of thrombin (green) and its aptamer (dark blue) by van der Waal forces. (For interpretation of the references to color in this figure legend, the reader is referred to the web version of the article.)

3. Results and discussion

3.1. Mechanism of thrombin-induced Apt-AuNPs aggregation

The Apt-AuNPs solutions changed color in the presence of thrombins (Scheme 1). At very low thrombin concentrations, no obvious aggregation was observed by naked eyes, presumably because interparticle cross-linking occured to only a very low degree. When the concentration of the thrombins was high enough to induce a greater degree of interparticle cross-linking, we observed aggregation of Apt-AuNPs to a greater extent (Scheme 1c). In this case, we believe that thrombin molecules act as bridges that link Apt-AuNPs together, with one thrombin molecule joining two Apt-AuNPs. At very high thrombin concentration, again, there was no obvious aggregation (Scheme 1d). The formation of cross-links decreased as a result of repulsion and steric effects because the surface of the Apt-AuNPs quickly became saturated with thrombin molecules through aptamer-thrombin binding. We even found that the thrombin-absorbed AuNPs which were saturated with thrombins were more stable than the Apt-AuNPs due to the Coulombic repulsion of negatively charged thrombins (The isoelectric point of thrombin shifted from 5.75 to 6.2 [45]).

To confirm the aptamer-AuNPs formation via covalent bond of Au—SH, the TEM analysis was performed. Herein, we compared TEM image of the gold nanoparticles modified by aptamers with a thiol at the end of 5′ with that of the gold nanoparticles modified by aptamers without a thiol group at the end of 5′ upon addition of thrombin. The images (figure S5a, b) illustrates that the gold nanoparticles modified by aptamers with a thiol tend to form the aggregation but the other does not upon adding 50 nM thrombins. This can be explained as follows: When there is no thiol at the 5′ end of the aptamer, the aptamers cannot be immobilized on the surface

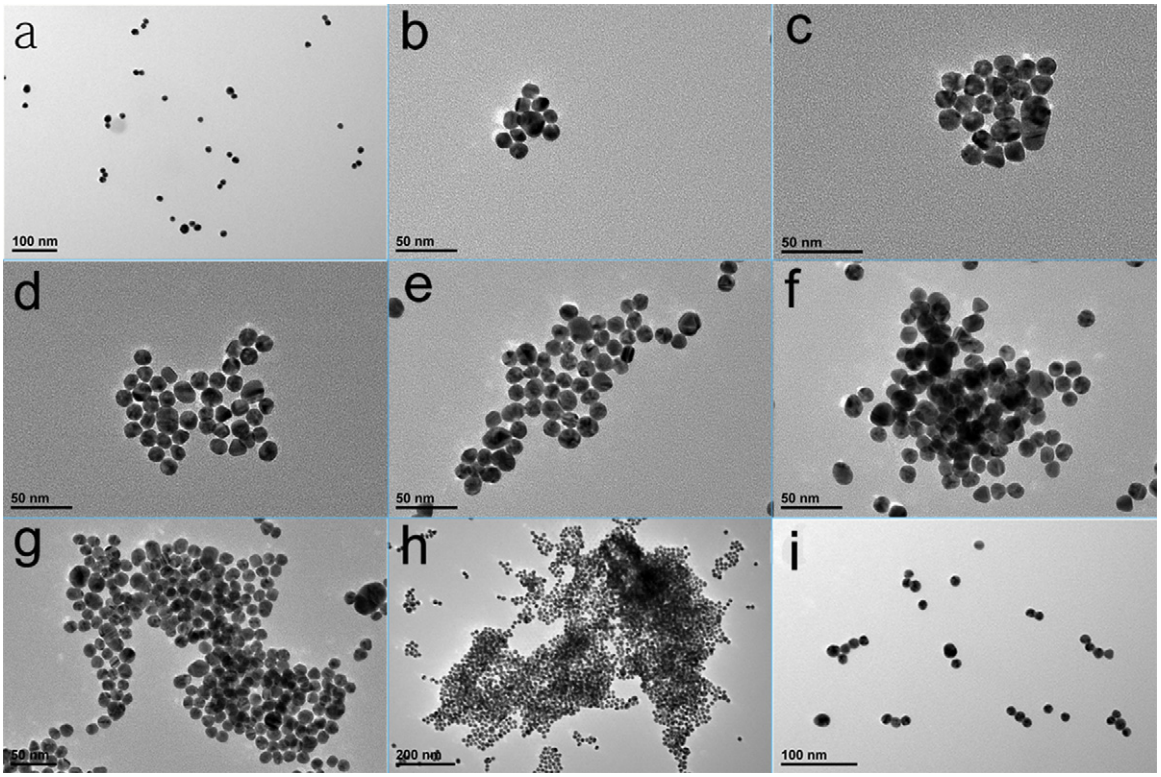

Fig. 1. TEM images of the nanoparticles obtained from the solutions containing Apt-AuNPs and thrombins. Thrombin concentrations: (a) 0, (b) 20 pM, (c) 50 pM, (d) 400 pM. (e) 1 nM, (f) 4 nM, (g) 20 nM, (h) 100 nM and (i) 500 nM. Particularly, we used 50 nM aptamer to modify the AuNPs in (b–d), and used 400 nM aptamer to modify the AuNPs in (f–i), respectively. We note that aggregation of the Apt-AuNPs occurred to the greater extend with higher concentration of thrombin. But the AuNPs aggregates dispersed upon adding more thrombin (up to 500 nM) to the solution.

of the AuNPs so the thrombin can only link two aptamers as it has two binding sites but cannot lead to the aggregate of the AuNPs. While, when there is a thiol on the 5′ end of the aptamer, the situation changed so that thrombins can act as bridges for the AuNPs because every gold nanoparticle was modified by many aptamers. This TEM comparison confirmed the formation of aptamer-AuNPs exactly. At the same time, we also provide UV–vis comparison data (figure S5c) to confirm the aptamer modified gold nanoparticles via Au—SH. We used aptamers with and without a thiol at the end of 5′ to modify the same AuNPs, and the spectrum show that there is a slight difference between the two solutions. However, when the thrombins were added to them, the situation changed. The AuNPs modified by aptamer with thiol aggregated seriously so that the absorbance at 520 nm had an obvious decrease while the other just decreased a little owing to the dilution effect of the addition of thrombin solution. We believed that this difference can confirm that the aptamer with a thiol was immobilized on the surface of the AuNPs efficiently and the other one was not. These UV–vis results are in great agreement with the TEM results we discussed earlier.

The proposed bridge structures could be confirmed by some UV–vis spectrum with wider wavelength range (figure S6). We compared the mixture of 50 μL AuNPs and 30 μL aptamer solution with the mixture of 50 μL AuNPs and 30 μL deionized water. The results show that the spectrum of the aptamer modified AuNPs had a peak at 260 nm (the arrows), which corresponds to the characteristic peak of DNA, whereas, the spectrum of AuNPs only does not show this peak. But both of them show the peak of AuNPs at 520 nm. After 1 nM and 100 nM thrombins were added to the Apta-AuNPs and incubated at 37°C for 30 min, the spectra changed obviously with the decreasing of absorbance at 520 nm. It is worth noting that the peak at 260 nm still exists, but a slight decrease and red shift can be observed when higher concentration of thrombin (100 nM) was added. We believe this decrease and red shift can be attributed to the formation of the proposed bridge structure, which leading to AuNPs aggregation.

3.2. Thrombin-induced aggregation

Owing to the characteristic surface plasmon resonance band of the monodispersed AuNPs at 520 nm [46,47], the dispersed Apt-AuNPs underwent red shifts with decreased absorbance at 520 nm whereas the absorbance at 600 nm increased upon aggregation. The absorbance at 520 and 600 nm were related to the quantities of the

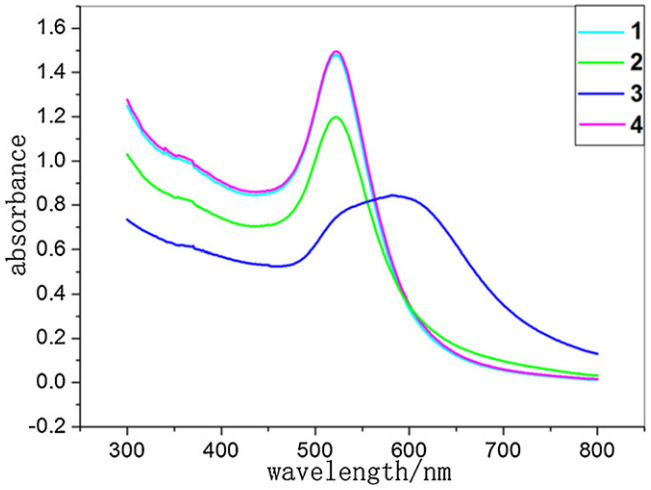

Fig. 2. UV–vis spectra of Apt-AuNPs in the presence of different concentrations of thrombins: (1) 0 nM; (2) 20 nM; (3) 100 nM; and (4) 500 nM. Absorbance at 520 nm decreased or shifted to higher wavelength slightly with increasing concentration of thrombin.

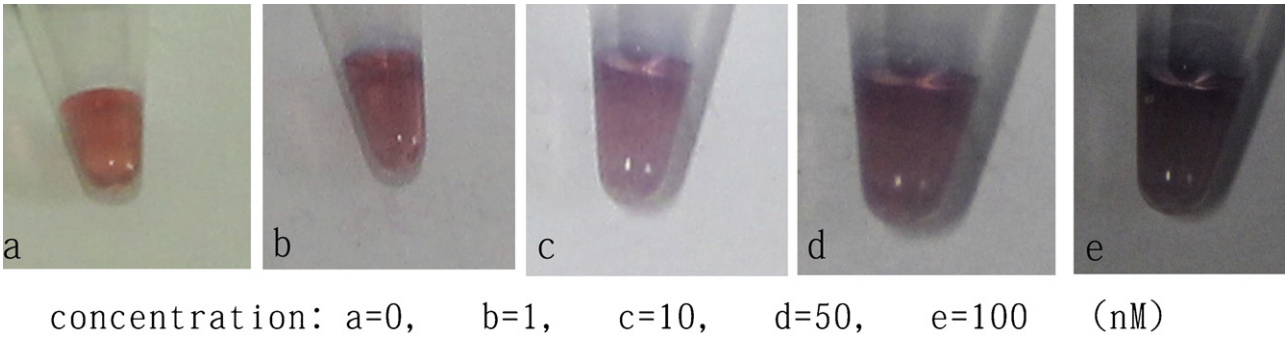

Fig. 3. Photographs of the Apt-AuNPs samples in the presence of different concentrations of thrombin: (a) 0 nM; (b) 1 nM; (c) 10 nM; (d) 50 nM; and (e) 100 nM. As the concentration of thrombin increased, the color changed from wine-red to blue-purple. (For interpretation of the references to color in this figure legend, the reader is referred to the web version of the article.)

dispersed and aggregated Apt-AuNPs respectively. As mentioned previously, the degree of aggregation depended on the thrombin concentration. At very high or very low thrombin concentrations, we observed no obvious aggregation (Fig. 1a and i and Fig. 2). Fig. 2 indicated that the absorbance at 520 nm decreased slightly at 20 nM and at 500 nM thrombins, with a distinct decrease in the absorbance at 520 nm that could be explained by the change in the dielectric constant of the AuNPs when its surface was largely covered with thrombin units. In the AuNPs solution, when the total concentration of thrombin was 100 nM, this value was much higher than that of the detection limit of thrombin by this approach (5 pM), and thus, serious aggregation was observed, and the peak at 520 nm decreased obviously. On the other hand, at very high concentrations (500 nM), there were enough thrombin molecules to bind to all aptamers on the AuNPs, therefore, less cross-linking formed (as shown in Scheme 1d). The aggregation was also monitored by TEM of various concentration of thrombin. As the Fig. 1 showed, the aggregation of the Apt-AuNPs occurred to the greater extend with the increasing of the thrombins, which can act as bridges for the Apt-AuNPs. We note that the AuNPs aggregates dispersed upon

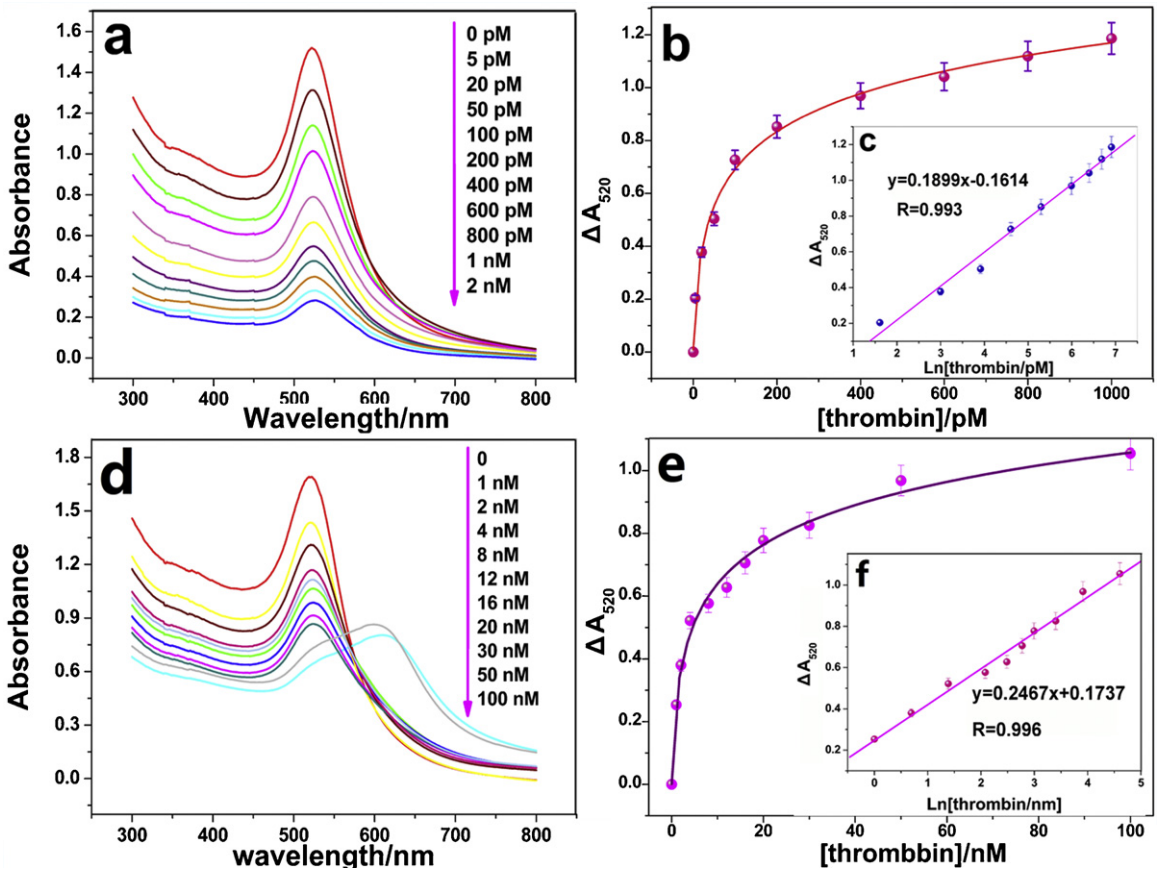

Fig. 4. The linear study of thrombin-induced Apt-AuNPs aggregation: (a–c) for the lower concentration of thrombin from 5 pM to 2 nM when using 50 nM aptamers to modify AuNPs. (a) The UV–vis absorbance spectra of Apt-AuNPs aggregate solution over the thrombin concentration of 5 pM–2 nM. (b) The peak absorbance change at 520 nm as a function of thrombin concentration; (inset c) the peak absorbance change of 520 nm is linear with logarithm of thrombin concentration over the range from 5 pM to 2 nM, and the linear function is $y = 0.1412x - 0.0164$ with $R = 0.993$. (d–f): Linear study for the higher concentration of thrombin from 1 nM to 100 nM, when using 400 nM aptamers to modify AuNPs. (d) The UV–vis absorbance spectra of Apt-AuNPs aggregate solution over the thrombin concentration of 1–100 nM; (e) the peak absorbance change at 520 nm as a function of thrombin concentration; (inset f) the peak absorbance change of 520 nm is linear with logarithm of thrombin concentration over the range from 1 nM to 100 nM, and the linear function is $y = 0.1685x + 0.176$.

adding more thrombin (up to 500 nM) to the solution (as shown in Fig. 1i) because of the repulsion and steric effects due to the saturated thrombin binding. On account of the Apt-AuNPs aggregation could be easily observed by naked eyes as the concentration of thrombin increased, the color changed from wine-red to blue-purple (as shown in Fig. 3). In this study, we used the absorbance peak at 520 nm to assess the degree of aggregation.

Fig. 4a and d displayed UV–vis absorbance spectra of the solutions containing Apt-AuNPs and thrombins over lower (5 pM–2 nM) and higher (1–100 nM) ranges respectively, revealing the evolution of aggregation. The aggregation of Apt-AuNPs induced by thrombins required 30 min to reach completion. When using 50 nM aptamer to modify AuNPs, the absorbance peak decreased to its minimum value at 2 nM thrombin (Fig. 4a), correspondingly, the absorbance change at 520 nm increased with the addition of thrombin (Fig. 4b), the results showed that ΔA_{520} was in very good linear relationship with the logarithm value of thrombin concentration with a correlation coefficient (R) of 0.993 in the range of 5 pM–2 nM (Fig. 4. inset c). Similarly, when using 400 nM aptamer to modify AuNPs, the absorbance peak decreased to its minimum value at 100 nM thrombin (Fig. 4d), correspondingly, the absorbance change increased upon thrombin addition (Fig. 4e), the results indicated that ΔA_{520} had very good linear relationship, again, with the logarithm value of thrombin concentration with R of 0.996 over the range of 1–100 nM (Fig. 4. inset f). More experimental results with different concentration of aptamers were shown in the supporting information. We point out that quantitative determination of the thrombins in the two different regions can be achieved by conducting a standard addition method. Based on above studies, the linear equation is obtained: $\Delta A_{520} = k_1 + k_2 \ln[\text{thrombin}]$ where, k_1 and k_2 are empirical constants which depend on the experimental conditions, such as the temperature, the preservation time of the AuNPs, the concentration of the aptamer and so on.

3.3. Specificity assays

Nonspecific binding is a critical issue when using nanomaterials for sensing macromolecules. The specificity of this method was determined by challenging it with other similar proteins: 10 nM lysozyme (Ly), 10 nM bovine hemoglobin (BHb) and 10 nM bovine serum albumin (BSA). As shown in Fig. 5a, the absorbance peaks of UV–vis spectra for the different proteins other than thrombin were only as small as the background, or even smaller than the background (in the absence of thrombin). We inferred that the proteins had no specific binding to the anti-thrombin aptamer, thus, no aggregation occurred. However, when we added 10 nM thrombin, the absorbance peak at 520 nm decreased obviously. In Fig. 5b, the value at the y-axis could be normalized by the absorbance peak decrease for thrombin versus background, the relative values of absorbance decrease were detected to be 4.5%, 5.3% and 6.7%, for Ly, BHb, and BSA, respectively (relative signal (%) = $(\Delta A_{520,\text{AuNPs}} - \Delta A_{520,\text{proteins}})/(\Delta A_{520,\text{AuNPs}} - \Delta A_{520,\text{thrombin}})$). This excellent selectivity arises from the high specificity of the anti-thrombin aptamer. In addition, the stability of this method for the detection of thrombin is also an important issue in practical applications. The stability of the approach was checked, and the results showed that the signal has only changed 2% after 2 h once interaction between thrombins and AuNPs completed (as shown in Fig. 6).

3.4. Real sample analysis

In real sample analysis, the complexity of serum may lead to the loss of selective interaction between the thrombin and the Apt-AuNPs, which would lead to no signal suppression at

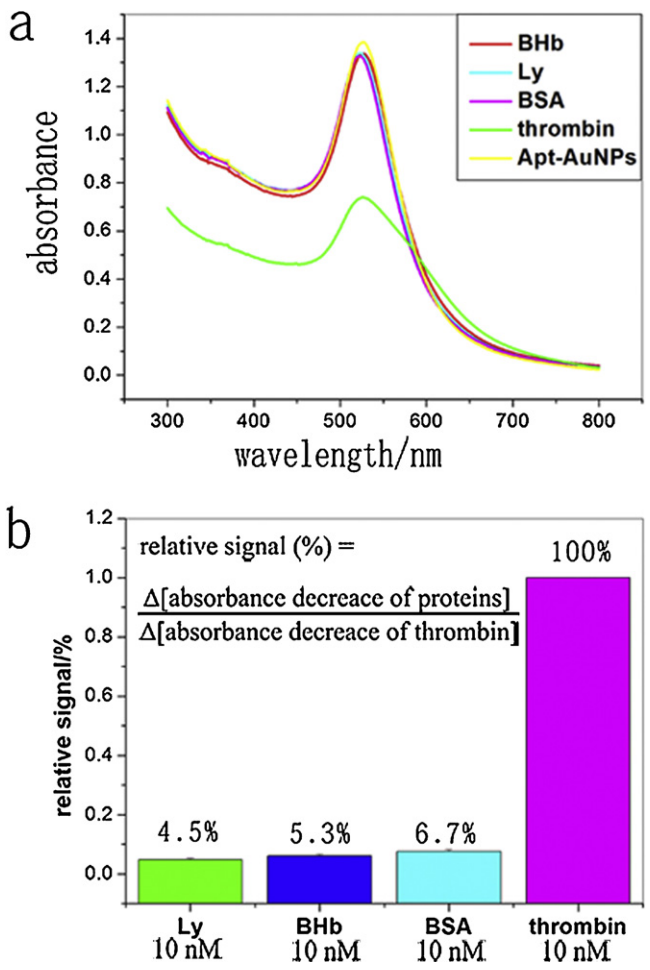

Fig. 5. Specificity assays. (a) The UV–vis spectra of Apt-AuNPs solution in the presence of different proteins. (b) The relative response of the sensing system to different proteins. The relative signal changes for other interferences are very small, indicating the excellent selectivity.

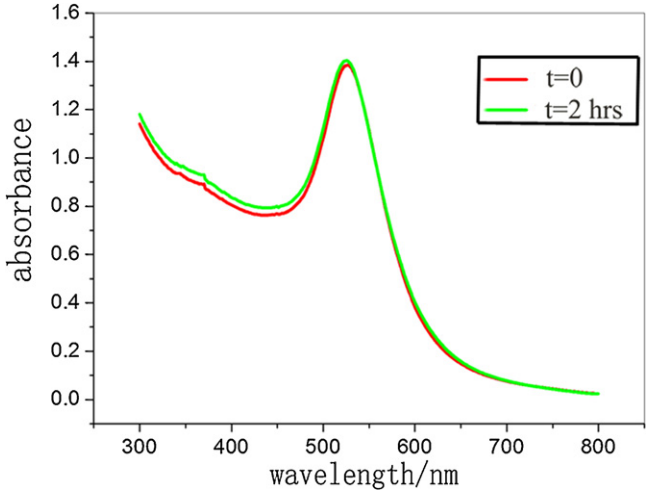

Fig. 6. The UV–vis spectra of Apt-AuNPs solution containing 10 nM thrombin at different time: $t = 0$ is the first record; and $t = 2$ h is the second record 2 h later. The small peak absorbance change indicates good stability of this method.

Table 2
Analytical results for thrombin in serum samples.

Serum sample[a]	Add (nmol/L)	Found (nmol/L)[b]	Recoveries (%)
1	0.040	0.041	102.5
2	0.100	0.097	97.0
3	0.500	0.476	95.2
4	1.000	0.964	96.4
5	5.000	5.158	103.2

[a] The serum sample was diluted 50 times.
[b] The average of five detections with this method.

520 nm. However, the experimental results showed that the signal suppression remained. Moreover, the real sample had been diluted 50 times before each experiment; thus, this large dilution was helpful to diminish false positive contributions from the matrix. To investigate if the method was applicable to real samples, we tested spiked serum samples with different thrombin concentrations; and the results were presented in Table 2. Because thrombin is not present in the blood and plasma of healthy subjects when coagulation is not occurring [33], the recoveries around 100% for spiked sample were expected. As shown in Table 2, the recoveries of standard addition were between 95.2%, and 103.2%, when using this method, which showed a satisfactory result. These results imply that this colorimetric method has a promising feature for the analytical application in complex biological samples.

4. Conclusion

This work introduces a very simple network assembly of Apt-AuNPs by thrombins, because thrombin has two binding sites for its aptamer, it can act as a bridge to link the monodispersed aptamer-modified gold nanoparticles together. As we know, the optical properties of gold nanoparticles are highly distance-dependent, which leads to the direct color change observed by naked eyes. And the exact concentration of thrombin can be determined by the absorbance change of AuNPs at 520 nm. The analytical results showed that the detection limit of 5 pM (1.679 ng/mL) could be achieved by this method. Moreover, the very good linear relationship could be obtained in two regions: 5 pM–2 nM (1.679–671.6 ng/mL) and 1–100 nM (335.8–33.58 μg/mL). Meanwhile, this colorimetric method exhibits excellent specificity, stability and applicability. The scope of the method presented here could be broad. The proposed strategy is expected to have wide applications in many other proteins, which have two binding sites for their aptamers.

Acknowledgment

This work was financially supported by National Natural Science Foundation of China (nos. 20903008, 20973019, and 50725208), Key Project Funding of NSFC of 50831001 and 20973019, NSFC for Outstanding Young Talents (507252008 and 10825419) and National 973 Program (2009CB623700). YP was supported by Students Research Training Program (SRTP).

Appendix A. Supplementary data

Supplementary data associated with this article can be found, in the online version, at http://dx.doi.org/10.1016/j.snb.2012.12.004.

References

[1] R. Elghanian, J.J. Storhoff, R.C. Mucic, R.L. Letsinger, C.A. Mirkin, Science 227 (1997) 1078–1081.
[2] S.E. Osborne, A.D. Eillington, Chemical Reviews 97 (1997) 349–370.
[3] C. Tuerk, L. Gold, Science 249 (1990) 505–510.
[4] K.C. Grabar, R.G. Freeman, M.B. Hommer, M.J. Natan, Analytical Chemistry 67 (1995) 735–743.
[5] R.C. Mucic, J.J. Storhoff, C.A. Mirkin, R.L. Letsinger, Journal of the American Chemical Society 120 (1998) 12674–12675.
[6] M.P.A. Ebert, S. Lamer, J. Meuer, P. Malfertheiner, M. Reymond, T. Buschmann, C. Röcken, V.J. Seibert, Proteome Research 4 (2005) 586–590.
[7] A. Oberbach, M. Blüher, H. Wirth, H. Till, P. Kovacs, Y. Kullnick, N. Schlichting, J.M. Tomm, U. Rolle-Kampczyk, J. Murugaiyan, H. Binder, A. Dietrich, M. von Bergen, Journal of Proteome Research 10 (2011) 4769–4788.
[8] K.M. Song, E. Jeong, W. Jeon, M. Cho, C. Ban, Analytical and Bioanalytical Chemistry 402 (2012) 2153–2161.
[9] Y.S. Kim, J.H. Kim, I.A. Kim, S.J. Lee, M.B. Gu, Biosensors and Bioelectronics 26 (2011) 4058–4063.
[10] J. Ji, J.R. Gan, J.L. Kong, P.Y. Yang, B.H. Liu, C. Ji, Electrochemistry Communications 16 (2012) 53–56.
[11] S. Chackalamannil, Journal of Medical Chemistry 49 (2006) 5389–5403.
[12] H.X. Chang, L.H. Tang, Y. Wang, J.H. Jiang, J.H. Li, Analytical Chemistry 82 (2010) 2341–2346.
[13] P. Pavlov, B. Shlyahovsky, I. Willner, Journal of the American Chemical Society 127 (2005) 6522–6523.
[14] J. Hu, P.C. Zheng, J.H. Jiang, G.L. Shen, R.Q. Yu, G.K. Liu, Analytical Chemistry 81 (2009) 87–93.
[15] H. Cho, B.R. Baker, S. Wachsmann-Hogiu, C.V. Pagba, T.A. Laurence, S.M. Lane, L.P. Lee, B.H.T. Jeffrey, Nano Letters 8 (2008) 4386–4390.
[16] L.D. Li, H.T. Zhao, Z.B. Chen, X.J. Mu, L. Guo, Analytical and Bioanalytical Chemistry 398 (2010) 563–570.
[17] C.Y. Deng, J.H. Chen, Z. Nie, M.D. Wang, X.C. Chu, X.L. Chen, X.L. Xiao, C.Y. Lei, S.Z. Yao, Analytical Chemistry 81 (2009) 739–745.
[18] Y. Du, B.L. Li, H. Wei, Y.L. Wang, E.K. Wang, Analytical Chemistry 80 (2008) 5110–5117.
[19] J.J. Storhoff, C.A. Mirkin, Chemical Reviews 99 (1999) 1849–1862.
[20] J.J. Storhoff, R. Elghanian, R.C. Mucic, C.A. Mirkin, R.L. Letsinger, Journal of the American Chemical Society 120 (1998) 1959–1964.
[21] C.A. Mirkin, R.L. Letsinger, R.C. Mucic, J. Storhoff, Journal of Nature 382 (1996) 607–609.
[22] X.D. Su, R. Kanjanawarut, Nano 3 (2009) 2751–2759.
[23] Baeissa, A. Dave, N. Smith, B.D. Liu, Journal of Applied Materials and Interfaces 2 (2010) 3594–3600.
[24] H. Deng, Y. Xu, Y.H. Liu, Z.J. Che, H.L. Guo, S.X. Shan, Y. Sun, X.F. Liu, K.Y. Huang, X.W. Ma, Y. Wu, X. Liang, Journal of Analytical Chemistry 84 (2012) 1253–1258.
[25] E. Tan, J. Jennifer Wong, D. Nguyen, Y. Zhang, B. Erwin, L.K.V. Ness, S.M. Baker, D.J. Galas, A. Niemz, Analytical Chemistry 77 (2005) 7984–7992.
[26] C.C. Huang, Y.F. Huang, Z.H. Cao, W.H. Tan, H.T. Chang, Analytical Chemistry 77 (2005) 5735–5741.
[27] S. Hong, I. Choi, S. Lee, Y.I. Yang, T. Kang, J. Yi, Journal of Analytical Chemistry 81 (2009) 1378–1382.
[28] L. Beqa, A.K. Singh, S.A. Khan, D. Senapati, S.R. Arumugam, P.C. Ray, Applied Materials and Interfaces 3 (2011) 668–673.
[29] J.S. Lee, P.A. Ulmann, M.S. Han, C.A. Mirkin, Nano Letters 8 (2008) 529–533.
[30] L.J. Ou, P.Y. Jin, X. Chu, J.H. Jiang, R.Q. Yu, Analytical Chemistry 82 (2010) 6015–6024.
[31] X.J. Xue, F. Wang, X.G. Liu, Journal of the American Chemical Society 130 (2008) 3244–3245.
[32] C.H. Li, J.M. Hu, T. Liu, S.Y. Liu, Macromolecules 44 (2011) 429–431.
[33] M.A. Shuman, P.W. Majerus, Journal of Clinical Investigation 58 (1976) 1249–1258.
[34] Y.L. Wang, H. Wei, B.L. Li, W. Ren, S.J. Guo, S.J. Dong, E.K. Wang, Chemical Communications (2007) 5220–5222.
[35] S.Y. Yan, R. Huang, Y.Y. Zhou, M. Zhang, M.G. Deng, X.L. Wang, X.C. Weng, X. Zhou, Chemical Communications 47 (2011) 1273–1275.
[36] C.W. Chi, Y.H. Lao, Y.S. Li, L.C. Chen, Biosensors and Bioelectronics 26 (2011) 3346–3352.
[37] J. Zhao, F.B. Lin, Y.H. Yi, Y. Yan Huang, H.T. Li, Y.Y. Zhang, S.H. Yao, Analyst 137 (2012) 3488–3495.
[38] T. Sun, L. Wang, N. Li, X.X. Gan, Bioprocess and Biosystems Engineering 34 (2011) 1081–1085.
[39] G.H. Liang, S.Y. Cai, P. Zhang, Y.Y. Peng, H. Chen, S. Zhang, J.L. Kong, Analytica Chimica Acta 689 (2011) 243–249.
[40] J. Turkevich, P.C. Stevenson, J. Hillie, Disscussions of the Faraday Society 5 (1951) 5–75.
[41] Y. Jiang, H. Zhao, Y.Q. Lin, N.N. Zhu, Y.R. Ma, L.Q. Mao, Angewandte Chemie International Edition 49 (2010) 4800–4804.
[42] D. Li, A. Wieckowska, I. Willner, Angewandte Chemie International Edition 47 (2008) 3927–3931.
[43] L. Strong, G.M. Whitesides, Langmuir 4 (1988) 546–558.
[44] R.G. Nuzzo, D.L. Allara, Journal of the American Chemical Society 105 (1983) 4481–4483.
[45] W.H. Seegers, L. Mccoy, R.K. Kipfer, G. Murano, Archives of Biochemistry and Biophyscis 128 (1968) 194–201.
[46] B. Dusemund, A. Hoffmann, T. Salzmann, U. Kreibig, G.Z. Schmid, Physics D 20 (1991) 305–308.
[47] U. Kreibig, Surface Science 156 (1985) 678–700.

Biographies

Yi Peng is currently doing his BS work at School of Chemistry and Environment, Beijing University of Aeronautics and Astronautics, Beijing.

Lidong Li received her PhD in analytical chemistry from Auburn University, USA, in 2005. She is currently working at School of Chemistry & Environment, Beijing University of Aeronautics and Astronautics, Beijing, as an associate professor. She studied in the area of electro-analytical chemistry. She is currently working toward electrochemical biosensors based on aptamer modification with nanomaterials amplification.

Xiaojiao Mu is currently doing her MS work at School of Chemistry and Environment, Beijing University of Aeronautics and Astronautics, Beijing.

Lin Guo received his PhD from Beijing Institute of Technology, Beijing, in 1997. He is currently working at School of Chemistry and Environment, Beijing University of Aeronautics and Astronautics, Beijing, as a professor. His research is focused on synthesis and characterization of nanomaterials, such as different transitional metal oxide nanomaterials, gold nanomaterials, and platinum nanomaterials.